Macromolecules

Article

pubs.acs.org/Macromolecules

Synthesis, Molecular and Photovoltaic Properties of Donor−Acceptor Conjugated Polymers Incorporating a New Heptacylic Indacenodithieno[3,2-*b*]thiophene Arene

Huan-Hsuan Chang, Che-En Tsai, Yu-Ying Lai, De-Yang Chiou, So-Lin Hsu, Chain-Shu Hsu, and Yen-Ju Cheng*

Department of Applied Chemistry, National Chiao Tung University, 1001 Ta Hsueh Road, Hsin-Chu, 30010 Taiwan

Supporting Information

ABSTRACT: We have developed a new multifused indacenodithieno[3,2-*b*]thiophene arene (**IDTT**) unit where the central phenylene is covalently fastened with the two outer thieno[3,2-*b*]thiophene (**TT**) rings, forming two cyclopentadiene rings embedded in a heptacyclic structure. This rigid and coplanar **IDTT** building block was copolymerized with electron-deficient acceptors, 4,7-dibromo-2,1,3-benzothiadiazole (**BT**), 4,7-dibromo-5,6-difluoro-2,1,3-benzothiadiazole (**FBT**) and 1,3-dibromo-thieno[3,4-*c*]pyrrole-4,6-dione (**TPD**) via Stille polymerization, respectively. Because the higher content of the thienothiophene moieties in the fully coplanar **IDTT** structure facilitates π-electron delocalization, these new polymers show much improved light-harvesting abilities and enhanced charge mobilities compared to **PDITTBT** copolymer using hexacyclic diindenothieno[3,2-*b*]thiophene (**DITT**) as the donor moieties. The device using **PIDTTBT**:$PC_{71}BM$ (1:4, w/w) exhibited a decent power conversion efficiency (PCE) of 3.8%. Meanwhile, the solar cell using **PIDTTFBT**:$PC_{71}BM$ (1:4 in wt %) blend exhibited a greater V_{oc} value of 0.9 V and a larger J_{sc} of 10.08 mA/cm^2, improving the PCE to 4.2%. The enhanced V_{oc} is attributed to the lower-lying of HOMO energy level of **PIDTTFBT** as a result of fluorine withdrawing effect on the **BT** unit. A highest PCE of 4.3% was achieved for the device incorporating **PIDTTTPD**:$PC_{71}BM$ (1:4 in wt %) blend.

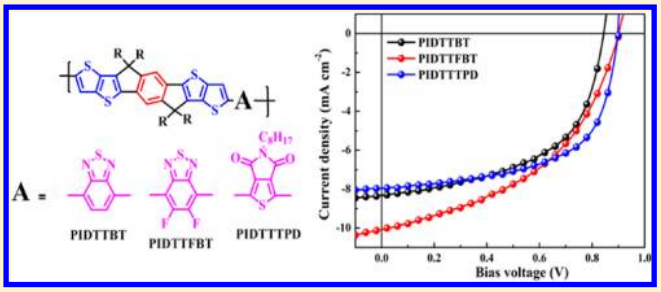

INTRODUCTION

Polymer solar cells (PSCs) using organic p-type (donor) and n-type (acceptor) semiconductors have attracted tremendous scientific and industrial interest.[1] The most critical challenge at molecular level is to develop p-type conjugated polymers that can simultaneously possess sufficient solubility for processability and miscibility with an n-type material, low band gap (LBG) for strong and broad absorption spectrum to capture more solar photons, and high hole mobility for efficient charge transport.[2] The most useful approach to make a LBG polymer is to connect electron-rich donor and electron-deficient acceptor segments along the conjugated polymer backbone. Thiophene and benzene aromatic rings are the most important ingredients to comprise p-type conjugated polymers. Benzene-based derivatives such as tricyclic 2,7-fluorene or 2,7-carbazole units have shown to serve as useful building blocks to construct donor−acceptor polymers having deep-lying HOMO energy levels that contribute to achieve high open-circuit voltage (V_{oc}) (>0.8 V) for PSCs.[3] However, the intrinsic drawback is that these polymers usually possess relatively large optical band gaps (>2 eV) that limit their ability to harvest sunlight and thus result in moderate short-circuit current (J_{sc}). On the other hand, because of the lower aromaticity to adapt more quinoidal resonance structure, thiophene-based D−A polymers have better light absorption ability to permit greater J_{sc}. However, their V_{oc} values are generally limited to ca. 0.6 V as a result of the high-lying HOMO levels.[4] Thieno[3,2-*b*]thiophene (**TT**) unit emerges as a superior thiophene-based building block to achieve high mobility p-type semiconductors.[5] This compact structure actually possesses higher aromatic stabilization energy than a thiophene, which can potentially lower the HOMO level for higher V_{oc}.[6] Moreover, the C_{2h} symmetry and coplanar geometry may promote more ordered packing and stronger interchain interactions to obtain exceptional hole mobility, which is beneficial for J_{sc}.[7] Introducing the alkyl chains into the two β-positions of thieno[3,2-*b*]thiophene unit is usually necessary to improve the solubility of the resulting polymers. Unfortunately, these side chains inevitably impose a negative effect on the effective conjugation due to severe steric hindrance-induced twisting between the neighboring aryls.[8] By implementing forced planarization via covalently fastening adjacent aromatic units in the polymer backbone, advantageous intrinsic properties such as reduced band gap and enhanced charge mobility can be retained.[9] Therefore, it is of interest to integrate benzene and thieno[3,2-*b*]thiophene units into a molecular entity with forced rigidification to simultaneously

Received: September 18, 2012
Revised: November 4, 2012
Published: November 27, 2012

dx.doi.org/10.1021/ma3019552 | *Macromolecules* 2012, 45, 9282−9291

extend the conjugation while maintaining the coplanarity. However, development of ladder-type architectures requires elegant molecular design and synthesis.[10] Recently, we first reported a multifused hexacyclic diindenothieno[3,2-*b*]-thiophene (**DITT**) unit, where the central **TT** ring is connected with two outer phenyl rings through two embedded cyclopentadienyl (**CP**) rings (Scheme 1).[11] This electron-rich unit

Scheme 1. Chemical Structures of Hexacyclic DITT and Heptacyclic IDTT Arenes and Their Corresponding Donor−Acceptor Copolymers

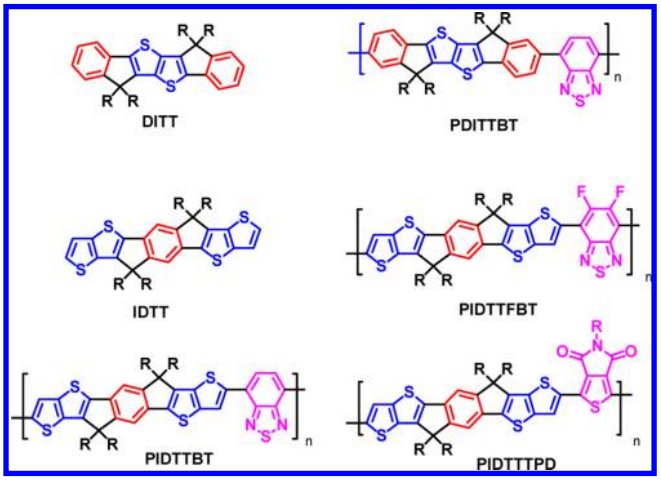

was copolymerized with electron-deficient benzothiadiazole acceptor to obtain a donor−acceptor copolymer **PDITTBT** (Scheme 1). Nevertheless, this polymer is short of absorption coverage at the visible and near IR region due to the fact that **DITT** possesses high content of high-aromaticity benzene rings (two benzene rings and one thieno[3,2-*b*]thiophene), leading to relatively large optical band gap and thus limited photocurrent. By reversing the arrangement of **TT** and benzene units in the **DITT** framework, we present here a new multifused heptacyclic structure, indacenodithieno[3,2-*b*]-thiophene (**IDTT**), where the central phenylene ring is fused with two outer **TT** rings by two carbon bridges. Compared to hexacyclic **DITT** unit, this heptacyclic **IDTT** has extended conjugation length with greatly increasing the content of the thiophene moieties (one benzene and two thieno[3,2-*b*]-thiophene units). Furthermore, the placement of the thienothiophene units at the two terminal sides of **IDTT** is advantageous for facile α-bromination or stannylation for subsequent polymerization. Four side chains introduced at the bridging carbons in **IDTT** guarantee solubility without twisting the coplanarity. Meanwhile, exploitation of suitable electron-deficient acceptors in combination with **IDTT** donor in the polymeric backbone is required. Benzothiadiazole (**BT**)[12] and thieno[3,4-*c*]pyrrole-4,6-dione (**TPD**)[13] are the widely used electron-deficient acceptors due to their suitable electron affinity and easy availability. 5,6-Difluorobenzothiadiazole (**FBT**) unit with two fluorine atoms on **BT** unit also emerges as a superior derivative for adjusting the molecular properties.[14] In this research, we report the detailed synthesis of the distannyl-**IDTT** monomer which was copolymerized with **BT**, **FBT**, **TPD** acceptor moieties to prepare a new class of D−A alternating **IDTT**-based copolymers (Scheme 1). Their thermal, optical and electrochemical properties have been carefully characterized. Preliminary results showed that the **IDTT**-based polymers are promising for photovoltaic solar cell applications.

Synthesis. The synthetic route for **Sn-IDTT** monomer is depicted in Scheme 2. Stille coupling of diethyl 2,5-dibromoterephthate with 2-(tributylstannyl)thieno[3,2-*b*]-thiophene yielded compound **1**. Double nucleophilic addition of the ester groups in **1** by (4-octyloxy)phenyl magnesium bromide led to the formation of benzylic alcohols in **2** which was subjected to intramolecular Friedel−Crafts cyclization under acidic condition to furnish the heptacyclic **IDTT** arene in a good yield of 81%. Bromination of **IDTT** by *N*-bromosuccinimide generated **Br-IDTT** in a high yield of 87%. Finally, **Br-IDTT** was lithiated by *n*-butyllithium followed by quenching with trimethyltin chloride to afford the distannyl

Scheme 2. Synthetic Route of Sn−IDTT Monomer

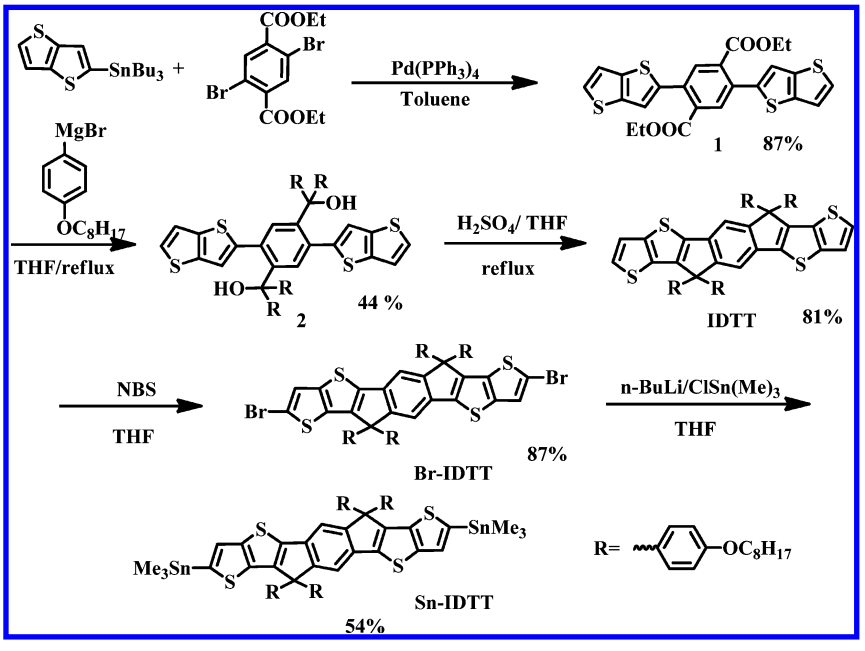

dx.doi.org/10.1021/ma3019552 | *Macromolecules* 2012, 45, 9282−9291

Sn-IDTT in a moderate yield of 54%. **Sn-IDTT** monomer was copolymerized with 4,7-dibromo-2,1,3-benzothiadiazole (**BT**), 4,7-dibromo-5,6-difluoro-2,1,3-benzothiadiazole (**FBT**) and 1,3-dibromo-thieno[3,4-*c*]pyrrole-4,6-dione (**TPD**) acceptor monomers via Stille coupling to afford three donor−acceptor copolymers, poly(indacenodithieno[3,2-*b*]thiophene-*alt*-benzothiadiazole) (**PIDTTBT**, M_n = 16.6 kDa, PDI = 1.7), poly(indacenodithieno[3,2-*b*]thiophene-*alt*-difluorobenzothiadiazole) (**PIDTTFBT**, M_n = 24.0 kDa, PDI = 1.2) and poly(indacenodithieno[3,2-*b*]thiophene-*alt*-thieno[3,4-*c*]-pyrrole-4,6-dione) (**PIDTTTPD**, M_n = 31.3 kDa, PDI = 2.0), respectively (Scheme 3). These copolymers purified by successive Soxhlet extraction and precipitation showed narrower molecular weight. The resulting copolymers flanked with four side chains on **IDTT** unit possess excellent solubilities in common organic solvents, such as chloroform, toluene, and THF.

Scheme 3. Synthesis of PIDTTBT, PIDTTFBT, and PIDTTTPD Copolymers

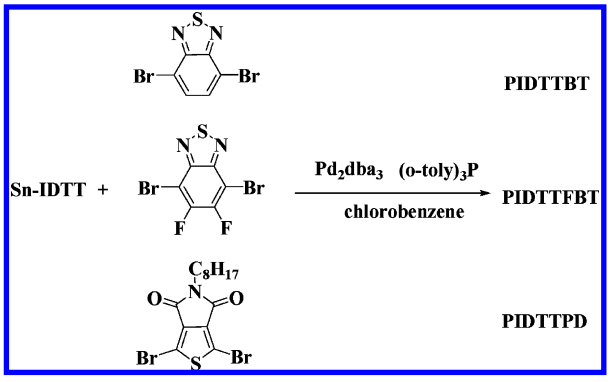

Thermal and Optical Properties. The thermal stability of the polymers was analyzed by thermogravimetric analysis (TGA) (Figure S1, Supporting Information). **PIDTTBT**, **PIDTTFBT**, and **PIDTTTPD** exhibited sufficiently high decomposition temperatures (T_d) of 414, 391, and 384 °C, respectively.

UV−vis absorption spectra of the three polymers in THF solutions and in thin films are shown in Figure 1 and the correlated optical parameters are summarized in Table 1. **PIDTTBT** and **PIDTTFBT** showed two obvious absorption bands in the spectra. The longer wavelength absorbance is attributed to the intramolecular charge transfer (ICT) between the electron-rich and the electron-deficient segments. However, the localized transition bands and ICT bands of **PIDTTTPD** overlap into a broad band covering the whole visible region from 400 to 700 nm, indicating that the accepting strength of **TPD** is weaker than that of **BT** unit. The absorption spectra of the three polymers shift toward longer wavelengths from the solution state to the solid state, indicating that the coplanar structure of **IDTT** is capable of inducing strong interchain interactions. The optical band gaps (E_g^{opt}) deduced from the onset of absorption in the solid state are determined to be 1.69 eV for **PIDTTBT**, 1.77 eV for **PIDTTFBT** and 1.95 eV for **PIDTTTPD**. Note that the optical band gap of **PDITTBT** is 2.15 eV, which is significantly larger than that of **PIDTTBT**, suggesting that the heptacyclic **IDTT** unit with higher content of thienothiophene moieties indeed facilitates the π-electron delocalization compared to the hexacyclic **DITT** unit.

Electrochemical Properties. Cyclic voltammetry (CV) was employed to examine the electrochemical properties and determine the highest occupied molecular orbital (HOMO) and lowest unoccupied molecular orbital (LUMO) energies of the polymers (Figure 2, Table 1). The three polymers showed stable and reversible p-doping and n-doping processes, which are important prerequisites for p-type semiconductor materials. The LUMO energy levels of **PIDTTBT**, **PIDTTFBT**, and **PIDTTTPD** are determined to be −3.40, −3.50, and −3.18 eV, respectively. The LUMO energy levels are higher than that of the $PC_{71}BM$ acceptor (−3.8 eV) to ensure energetically favorable electron transfer. It should be noted that the HOMO energy of **PIDTTFBT** (−5.30 eV) is lower than that of **PIDTTBT** (−5.43 eV) due to the two electron-withdrawing fluorine atoms on the **BT** units.[14] Furthermore, **PIDTTTPD** shows the lowest HOMO energy level of −5.45 eV, indicating that **TPD** acceptor unit is also capable of lowering the HOMO energy level of the resulting polymer. The HOMO energy levels are within the ideal range to ensure better air-stability and greater attainable V_{oc}.

Theoretical Calculations. In order to gain more insight into the molecular orbital properties of the polyaromatic π-electron systems, quantum−chemical calculations were performed with the Gaussian09 suite employing the B3LYP and TD-B3LYP density functionals in combination with the 6-311G(d,p) basis set. Considering an insignificant effect on

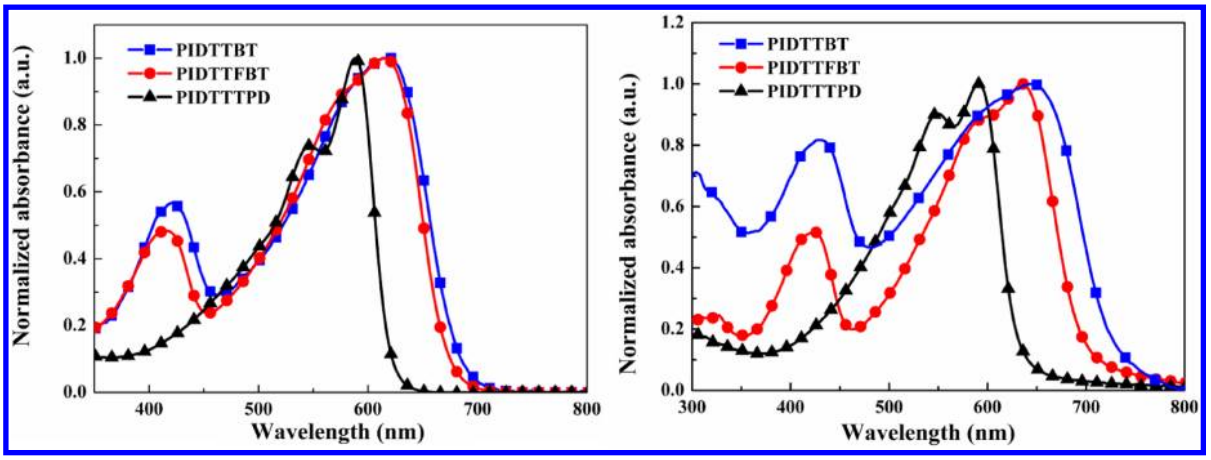

Figure 1. Normalized absorption spectra of **PIDTTBT**, **PIDTTFBT**, and **PIDTTTPD** in (a) THF solutions and (b) in thin films.

dx.doi.org/10.1021/ma3019552 | *Macromolecules* 2012, 45, 9282−9291

Table 1. Summary of the Intrinsic Properties of the Polymers[a]

polymer	M_n (kDa)	PDI	T_d (°C)	E_g^{opt} (eV) (Film)	λ_{max} (nm) THF	λ_{max} (nm) film	HOMO (eV)	LUMO(eV)
PIDTTBT	16.6	1.7	414	1.69	420	430	−5.30	−3.40
					622	645		
PIDTTFBT	24.0	1.2	391	1.77	415	424	−5.43	−3.50
					616	635		
PIDTTTPD	31.3	2.0	384	1.95	588	591	−5.45	−3.18

[a] E_g^{opt} from the onset of UV spectra in thin film.

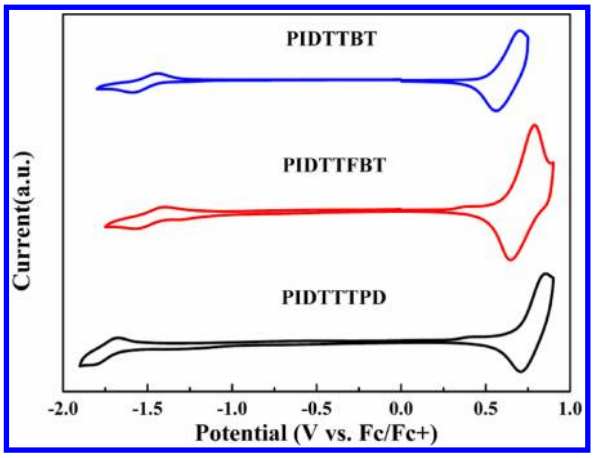

Figure 2. Cyclic voltammograms of **PIDTTBT**, **PIDTTFBT**, and **PIDTTTPD** in the thin films at a scan rate of 50 mV/s.

electronic properties, all the side-chain substituents were replaced with methyl groups for simplicity. Repeating units, denoted as **IDTTBT**, **IDTTFBT**, and **IDTTTPD**, in their most stable conformations were used as simplified model compounds for **PIDTTBT**, **PIDTTFBT**, and **PIDTTTPD**, respectively.

The calculated HOMO/LUMO energy, excitation energy, oscillator strength, and configurations of the excited states are summarized in Table 2 and the frontier orbitals, HOMO (H), LUMO (L) and the closeby LUMO+1 (L+1) are illustrated in Table 3. The HOMO electron density distribution of **IDTTTPD** is analogous to that of **IDTTFBT** and **IDTTBT**, where the electron density is not only distributed homogeneously along the molecular backbone of the **IDTT** moiety but also on parts of the acceptor. Given that the contribution of the **IDTT** moiety to the HOMO energy level should be similar among the three compounds, the difference in the HOMO energy level therefore mainly depends on the nature of the acceptors. Consistent with the electrochemical experiments, the calculated HOMO energy levels of the three model compounds follow the order: **IDTTTPD** (−5.25 eV) < **IDTTFBT** (−5.23 eV) < **IDTTBT** (−5.18 eV). On the contrary, the LUMO of **IDTTTPD** is higher in energy than that of **IDTTFBT** and **IDTTBT**. **IDTTFBT** and **IDTTBT** have similar LUMO electron density patterns of which the electron density is mainly located on the acceptors (**BT** and **FBT**). Instead, the electron density of LUMO in **IDTTTPD** is not only localized on **TPD** unit but span from **TPD** to **IDTT** moieties. Involvement of the **IDTT** orbitals in the LUMO of **IDTTTPD** may result in a high-lying energy level of LUMO.

Table 2. Calculated[a] HOMO/LUMO Energy, Excitation Energy, Oscillator Strength, and Configurations (with Large CI Coefficients) of the Excited States

compound	HOMO (eV)	LUMO (eV)	excitation energy $\lambda_{max,exp}$ (nm)[b]	excitation energy λ_{calcd} (nm)	oscillator strength	symmetry	configuration[c]
IDTT	−5.22	−1.87	393, 417	420	1.1262	singlet-A	**H→L**
				321	0.2295	singlet-A	**H−4→L**
							H→L+2
IDTTBT	−5.18	−2.78	622	597	0.6822	singlet-A	**H→L**
			420	433	0.7493	singlet-A	H−1→L
				430	0.315	singlet-A	**H→L+1**
							H−1→L
							H→L+1
							H−2→L
IDTTFBT	−5.23	−2.89	616	607	0.6499	singlet-A	**H→L**
			415	435	0.2193	singlet-A	H−3→L
							H−2→L
							H−1→L
							H→L+1
				431	0.8399	singlet-A	**H→L+1**
							H−3→L
							H−2→L
							H−1→L
IDTTTPD	−5.25	−2.53	588	521	1.4519	singlet-A	**H→L**

[a] TD−B3LYP/6-311G(d,p), PCM=THF. [b] Experimental values were measured for nonsimplified **IDTT**, **IDTTBT**, **IDTTFBT**, **IDTTTPD** in THF solution, respectively. [c] Configurations with largest coefficients in the CI expansion of each state are highlighted in boldface.

dx.doi.org/10.1021/ma3019552 | *Macromolecules* 2012, 45, 9282−9291

Table 3. Plots (Isovalue = 0.02 au) of Frontier Orbitals of IDTT, IDTTBT, IDTTFBT, and IDTTPD Calculated at the Level of B3LYP/6-311G(d,P) in THF

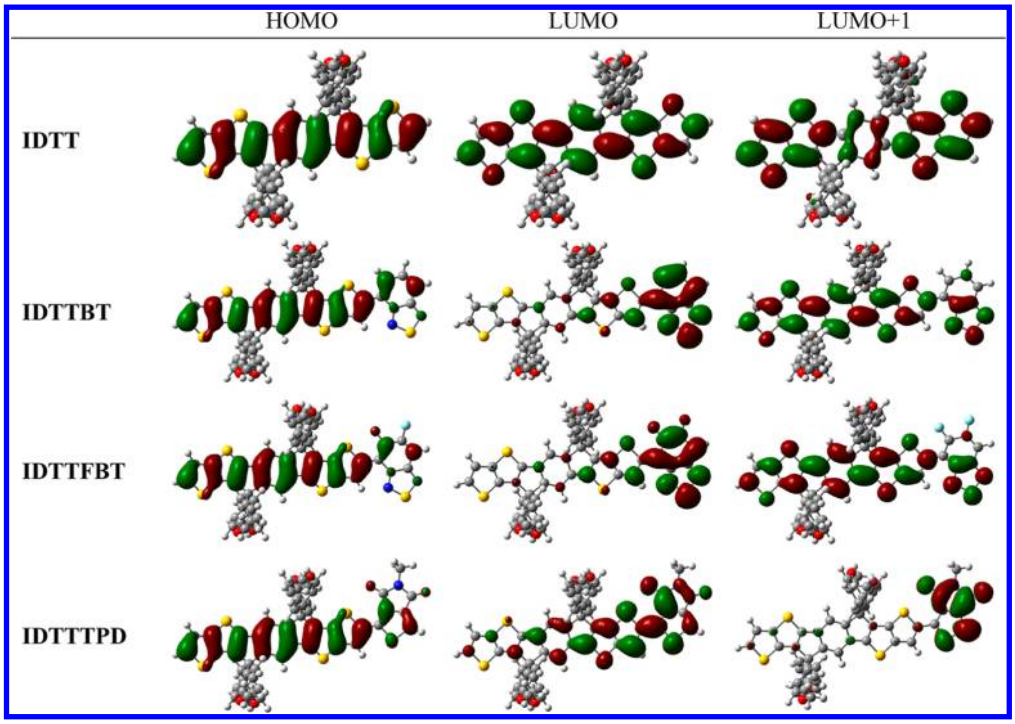

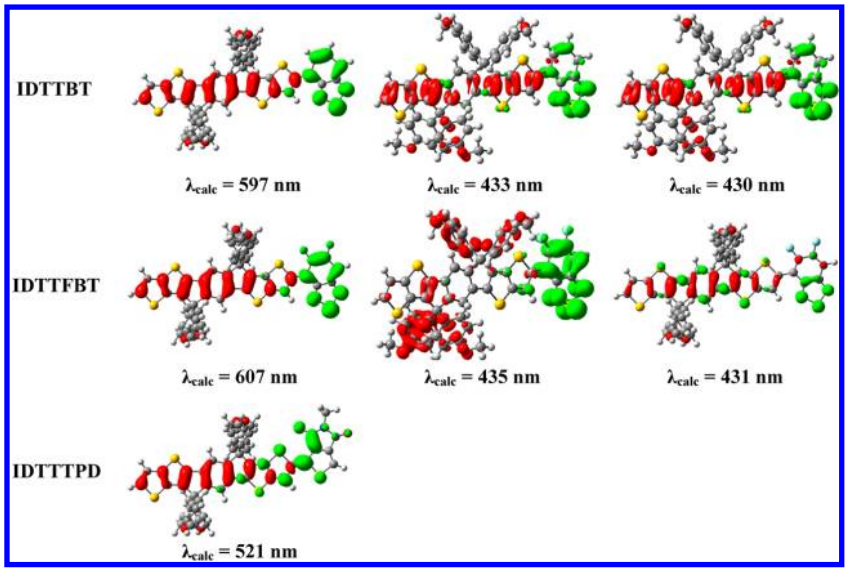

Figure 3. Electron density difference maps (EDDMs) of selected singlet electronic transitions of **IDTTBT** (at 597, 433, and 430 nm), **IDTTFBT** (at 607, 435, and 431 nm), and **IDTTTPD** (at 521 nm). Red indicates a decrease in charge density, while green indicates an increase. All EDDMS were plotted with isovalue 0.0012 au.

As listed in Table 2, although there are variations in the absolute values, the calculated absorptions are still in good agreement with the experimental values. In order to have further understanding of these electronic transitions, electron density difference maps (EDDMs) were conducted (Figure 3).[15] The electronic transitions can therefore be visualized through EDDMs. Red indicates a decrease in charge density, while green indicates an increase. For **IDTTBT**, the lowest energy singlet electronic transition (λ_{calc} = 597 nm; $\lambda_{max,exp}$ = 622 nm) indicates a pronounced intramolecular charge transfer (ICT) from **IDTT** to **BT**. The transitions at λ_{calc} = 433 and 430 nm are close in energy and may not be separable. In fact, in the UV absorption spectrum, only one absorption peak ($\lambda_{max,exp}$= 420 nm) was observed. On the basis of the EDDMs, both transitions belong to charge separations from the molecular backbone of **IDTT** and one 4-methoxyphenyl side chain to the **BT** unit. The lowest energy singlet electronic transition (λ_{calc} = 607 nm; $\lambda_{max,exp}$= 616 nm) of **IDTTFBT** is a ICT band, which is basically caused by the electron transfer from **IDTT** to **FBT**. The transitions at λ_{calc} = 435 and 431 nm are also inseparable in the experimental spectrum ($\lambda_{max,exp}$= 415 nm). One at λ_{calc} = 435 nm is assigned to the ICT from the flanking 4-methoxyphenyl groups of **IDTT** to **BT**, and the other one at λ_{max} = 431 nm only occurs at localized regions. Lastly, the most

dx.doi.org/10.1021/ma3019552 | *Macromolecules* 2012, 45, 9282−9291

Table 4. FET Characteristics of the Polymer Thin Films

polymer	SAM layer	annealing temperature (°C)	mobility ($cm^2\ V^{-1}\ s^{-1}$)	on/off	V_t (V)
PIDTTBT	**ODTS**	200	7×10^{-3}	1.9×10^3	−13.8
PIDTTFBT	**ODTS**	150	1×10^{-2}	1.4×10^7	−21.7
PIDTTTPD	**ODTS**	200	1×10^{-3}	3.2×10^4	−25.4

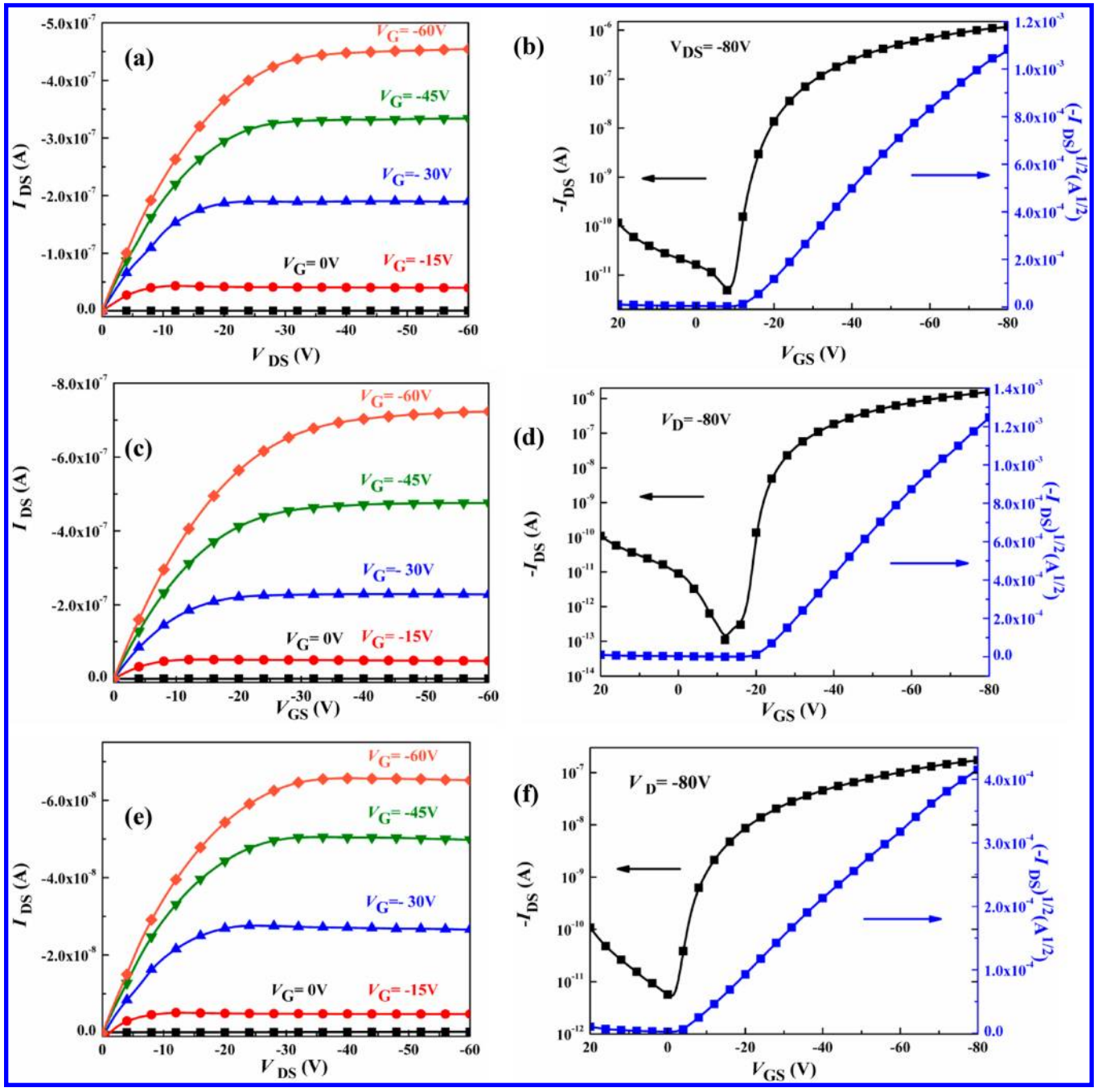

Figure 4. . Typical output curves (a, c, e) and transfer plots (b, d, f) of the OFET devices based on **PIDTTBT**, **PIDTTFBT**, and **PIDTTTPD**, respectively, with ODTS-SAM layer.

probable vertical excitation of **IDTTTPD** is calculated to be 521 nm, which deviates slightly from the $\lambda_{max,exp}$ of 589 nm. It mainly results from the ICT from **IDTT** to **TDP** and the $\pi-\pi^*$ transition within the **IDTT** unit has a minor contribution.

Organic Field Effect Transistors. To investigate the mobilities of the polymers, organic field-effect transistors (OFETs) were fabricated in the bottom-contact/top-contact geometry as described in the Experimental Section (Table 4 and Figure 4). The hole mobilities were deduced from the transfer characteristics of the devices in the saturation regime. The polymers-based OFETs using SiO_2 as gate dielectric was treated with octadecyltrichlorosilane (ODTS) to form a self-assembly monolayer (SAM). With the modification of a ODTS-SAM layer along with annealing temperature at 150

dx.doi.org/10.1021/ma3019552 | *Macromolecules* 2012, 45, 9282−9291

and 200 °C, the hole mobilities of the three polymers were determined to be 7×10^{-3} cm^2 V^{-1} s^{-1}, 1×10^{-2} cm^2 V^{-1} s^{-1}, and 1×10^{-3} cm^2 V^{-1} s^{-1} with the on−off ratios of 1.9×10^3, 1.4×10^7, and 3.2×10^4 for **PIDTTBT**, **PIDTTFBT**, and **PIDTTTPD** devices, respectively. It should be mentioned that **PDITTBT** using hexacyclic **DITT** as the donor showed a much lower mobility of 7×10^{-5} cm^2 V^{-1} s^{-1}.[11] This result again indicates that higher content of thienothiophene unit can improve the charge transporting properties.

Photovoltaic Characteristics. Bulk heterojunction photovoltaic cells were fabricated by spin-coating the blends from *o*-dichlorobenzene solutions at various polymer-to-$PC_{71}BM$ ratios on the basis of ITO/PEDOT:PSS/polymer:$PC_{71}BM$/Ca/Al configuration and their performances were measured under a simulated AM 1.5 G illumination of 100 mW/cm^2. The asymmetric $PC_{71}BM$ was used due to its stronger light absorption in the visible region than that of $PC_{61}BM$. The characterization data are summarized in Table 5 and the *J*−*V* curves of these polymers are shown in Figure 5. The blend ratio of the active layers shown in the Table 5 is the result of the optimized conditions for the devices. The device based on the **PIDTTBT**:$PC_{71}BM$ (1:4 in wt %) blend exhibited a V_{oc} of 0.84 V, a J_{sc} of 8.32 mA/cm^2, a FF of 55%, delivering a decent PCE of 3.8%. It is noteworthy that the device based on **PDITTBT** polymer using the hexacyclic **DITT** unit as the donor only exhibited a lower V_{oc} of 0.88 V, a J_{sc} of 7.46 mA/cm^2, resulting in a lower PCE of 2.7%.[11] Meanwhile, the device using **PIDTTFBT**:$PC_{71}BM$ (1:4 in wt %) blend exhibited a greater V_{oc} value of 0.9 V and a larger J_{sc} of 10.08 mA/cm^2 with an improved PCE to 4.2%. The enhanced V_{oc} is attributed to the lower-lying of HOMO energy level of **PIDTTFBT** as a result of fluorine withdrawing effect on the FBT unit. More encouragingly, the device based on the **PIDTTTPD**:$PC_{71}BM$ (1:4 in wt %) blend exhibited a high V_{oc} of 0.90 V, a J_{sc} of 7.99 mA/cm^2, a FF of 60%, leading to a highest PCE of 4.3%. Even though the device derived from **PIDTTFBT** has the highest V_{oc} and J_{sc}, it does not show a better PCE than the **PIDTTTPD**-based device, which is due to the fact that the device of **PIDTTTPD** has a much larger FF than that of **PIDTTBT**. To confirm the accuracy of the measurements of the devices, the corresponding external quantum efficiency (EQE) spectra were measured under illumination of monochromatic light (Figure 4). The J_{sc} values calculated from integration of the EQE spectra agree well with the J_{sc} obtained from the *J*−*V* measurements.

Table 5. PSCs Characteristics

polymer	blend ratio polymer:$PC_{71}BM$	V_{oc} (V)	J_{sc} (mA/cm^2)	FF (%)	PCE (%)
PIDTTBT	1: 4	0.84	8.32	55	3.8
PIDTTFBT	1: 4	0.90	10.08	46	4.2
PIDTTTPD	1: 4	0.90	7.99	60	4.3

CONCLUSIONS

Compared to thiophene unit, C_{2h}-symmetry thieno[3,2-*b*]-thiophene (**TT**) unit with higher aromatic stabilization energy and coplanar geometry is a promising building block for donor−acceptor conjugated polymers to obtain higher V_{oc} and J_{sc}. However, introducing aliphatic side chains on the *β*-positions of **TT** units leads to severe steric hindrance-induced twisting between the neighboring aryls in the polymer backbone. A straightforward approach to circumvent this deficiency is to embed **TT** units in a multifused ladder-type structure. A hexacyclic diindenothieno[3,2-*b*]thiophene (**DITT**) unit has been first developed. Nevertheless, **DITT** possesses high content of high-aromaticity benzene rings resulting in relatively large optical band gap and thus limited J_{sc}. By reversing the arrangement of **TT** and benzene units in the **DITT** framework, we have successfully developed a new multifused heptacyclic structure, indacenodithieno[3,2-*b*]-thiophene (**IDTT**), where the central phenylene ring is fused with two outer **TT** rings. The ladder-type **IDTT** framework can be easily constructed by Friedel−Crafts annulation. The optical and electrochemical properties of the resulting polymers have been characterized experimentally and theoretically. Compared to the hexacyclic **DITT** unit, this heptacyclic **IDTT** has extended conjugation length with significantly increasing the content of the thiophene moieties. Because of the more favorable *π*-electron delocalization, **IDTT**-based polymers show much improved light-harvesting abilities and enhanced charge mobilities. The device using **PIDTTBT**:$PC_{71}BM$ (1:4, w/w) blend exhibited an improved efficiency of 3.8%. Meanwhile, the device using **PIDTTFBT**:$PC_{71}BM$ (1:4, w/w) blend exhibited a greater V_{oc} value of 0.9 V as a result of the fluorine withdrawing effect on the **BT** unit, and a larger J_{sc} of 10.08 mA/cm^2 with a higher PCE of 4.2%. The device based on the

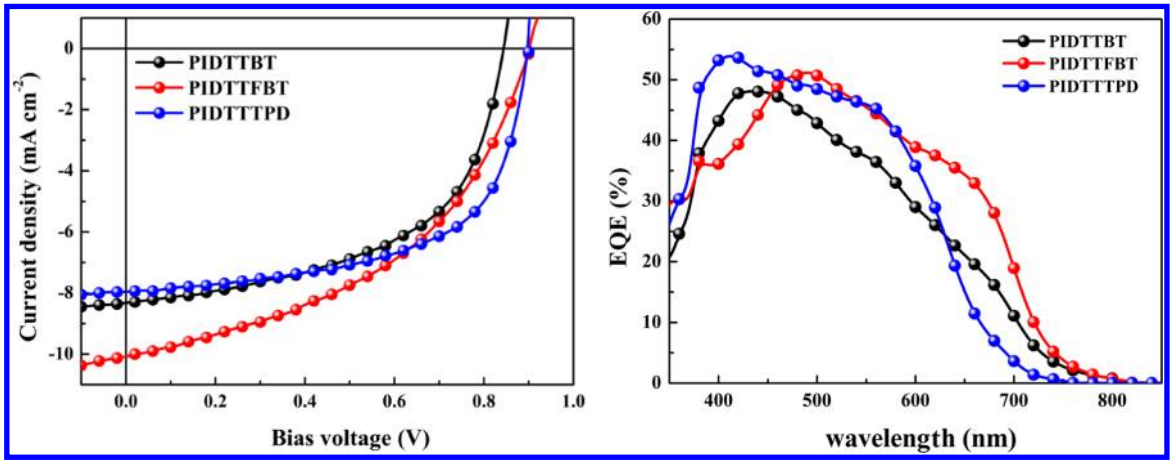

Figure 5. *J*−*V* characteristics of ITO/PEDOT:PSS/polymer:$PC_{71}BM$/Ca/Al under illumination of AM1.5, 100 mW/cm^2, and corresponding EQE spectra.

dx.doi.org/10.1021/ma3019552 | *Macromolecules* 2012, 45, 9282−9291

PIDTTTPD:$PC_{71}BM$ (1:4 in wt %) blend exhibited a high V_{oc} of 0.90 V and a highest PCE of 4.3%. We envisage that further improvement of device performance is highly achievable by optimizing the processing conditions which are underway in our laboratories. This research demonstrated that the new heptacyclic indacenodithieno[3,2-*b*]thiophene is one of the most promising building blocks for constructing high-performance conjugated polymers.

EXPERIMENTAL SECTION

General Measurement and Characterization. All chemicals are purchased from Aldrich or Acros and used as received unless otherwise specified. ^1H and ^{13}C NMR spectra were measured using Varian 300 and 400 MHz instrument spectrometers. Thermogravimetric analysis (TGA) was recorded on a Perkin-Elmer Pyris under nitrogen atmosphere at a heating rate of 10 °C/min. Absorption spectra were recorded on a HP8453 UV−vis spectrophotometer. The molecular weight of polymers was measured on a Viscotek VE2001GPC, and polystyrene was used as the standard (THF as the eluent). The electrochemical cyclic voltammetry (CV) was conducted on a CH Instruments Model 611D. A carbon glass coated with a thin polymer film was used as the working electrode and Ag/Ag^+ electrode as the reference electrode, while 0.1 M tetrabutylammonium hexafluorophosphate (Bu_4NPF_6) in acetonitrile was the electrolyte. CV curves were calibrated using ferrocence as the standard, whose oxidation potential is set at −4.8 eV with respect to zero vacuum level. The HOMO energy levels were obtained from the equation HOMO = $-(E_{ox}{}^{onset} - E_{(ferrocene)}{}^{onset} + 4.8)$ eV. The LUMO levels of polymer were obtained from the equation LUMO = $-(E_{red}{}^{onset} - E_{(ferrocene)}{}^{onset} + 4.8)$ eV.

OFET Fabrication. An n-type heavily doped Si wafer with a SiO_2 layer of 300 nm and a capacitance of 11 nF/cm^2 was used as the gate electrode and dielectric layer. Thin films (40−60 nm in thickness) of polymers were deposited on octadecyltrichlorosilane (ODTS)-treated SiO_2/Si substrates by spin-coating their *o*-dichlorobenzene solutions (5 mg/mL). Then, the thin films were annealed at different temperatures (150 or 250 °C) for 30 min. Gold source and drain contacts (40 nm in thickness) were deposited by vacuum evaporation on the organic layer through a shadow mask, affording a bottom-gate, top-contact device configuration. Electrical measurements of OTFT devices were carried out at room temperature in air using a 4156C, Agilent Technologies. The field-effect mobility was calculated in the saturation regime by using the equation $I_{ds} = (\mu WC_i/2L)(V_g - V_t)^2$, where I_{ds} is the drain-source current, μ is the field-effect mobility, W is the channel width (1 mm), L is the channel length (100 μm), C_i is the capacitance per unit area of the gate dielectric layer, V_g is the gate voltage, and V_t is threshold voltage.

PSCs Fabrication. ITO/Glass substrates were ultrasonically cleaned sequentially in detergent, water, acetone and iso-propanol (IPA). The cleaned substrates were covered by a 30 nm thick layer of PEDOT:PSS (Clevios P provided by Stark) by spin coating . After annealing in a glovebox at 150 °C for 30 min, the samples were cooled to room temperature. Polymers were dissolved in *o*-dichlorobenzene (ODCB), and then $PC_{71}BM$ (purchased from Nano-C) was added. The solution was then heated at 80 °C and stirred overnight at the same temperature. Prior to deposition, the solution were filtered (0.45 μm filters). The solution of polymer:$PC_{71}BM$ was then spin coated to form the active layer. The cathode made of calcium (35 nm thick) and aluminum (100 nm thick) was sequentially evaporated through a shadow mask under high vacuum ($<10^{-6}$ Torr). Each sample consists of 4 independent pixels defined by an active area of 0.04 cm^2. Finally, the devices were encapsulated and characterized in air.

Synthesis of Compound 1. A mixture of diethyl 2,5-dibromoterephthalate (6.05 g, 15.9 mmol), 2-(tributylstannyl)thieno-[3,2-*b*]thiophene (15.71 g, 36.6 mmol), $Pd(PPh_3)_4$ (0.74 g, 0.6 mmol), and degassed toluene (80 mL) was heated to 130 °C under nitrogen atmosphere for 16 h. The reaction mixture was poured into water (150 mL) and extracted with ethyl acetate (300 mL × 3). The combined organic layer was dried over $MgSO_4$ and the solvent was removed *in vacuo*. The residue was purified by column chromatography on silica gel (hexane/ethyl acetate, v/v, 20/1) and then recrystallized from hexane to give a light yellow solid **1** (6.9 g, 87%): ^1H NMR ($CDCl_3$, 300 MHz, ppm) δ 1.13 (t, J = 7.1 Hz, 6 H), 4.21−4.28 (q, J = 7.1 Hz, 4 H), 7.26−7.29 (m, 4 H), 7.40 (d, J = 5.1 Hz, 2 H), 7.89 (s, 2 H); ^{13}C NMR ($CDCl_3$, 75 MHz, ppm) δ 13.8, 61.8, 119.3, 119.4, 127.4, 132.0, 133.8, 134.1, 139.3, 139.9, 142.0, 167.4; MS (EI, $M^{+\bullet}$, $C_{24}H_{18}O_4S_4$) calcd 498.01, found 498.

Synthesis of Compound 2. A Grignard reagent was prepared by the following procedure. To a suspension of magnesium turnings (3.2 g, 132.0 mmol) and 3−4 drops of 1,2-dibromoethane in dry THF (120 mL) was slowly added 1-bromo-4-(octyloxy)benzene (34.23 g, 120.0 mmol) dropwise and the mixture was then stirred for 1 h. To a THF (50 mL) solution of **1** (4.80 g, 9.6 mmol) under nitrogen atmosphere was added dropwise the freshly prepared 4-(octyloxy)phenyl-1-magnesium bromide (1 M, 76.8 mL, 76.8 mmol) at room temperature. The resulting mixture was heated at the refluxing temperature for 16 h, cooled to room temperature, poured into water (100 mL), and extracted with ethyl acetate (150 mL × 3). The collected organic layer was dried over $MgSO_4$. After removal of the solvent under reduced pressure, the residue was purified by column chromatography on silica gel (hexane/ethyl acetate, v/v, 30/1) to furnish a yellow solid **2** (5.17 g, 43.7%): ^1H NMR ($CDCl_3$, 300 MHz, ppm) δ 0.88, (t, J = 6.8 Hz, 12 H), 1.28−1.45 (m, 40 H), 1.75−1.80 (m, 8 H), 3.42 (s, 2 H), 3.94 (t, J = 6.6 Hz, 8 H), 6.27 (s, 2 H), 6.80 (d, J = 9 Hz, 8 H), 6.90 (s, 2 H), 7.08 (d, J = 9 Hz, 8 H), 7.13 (d, J = 5.1 Hz, 2 H), 7.30 (d, J = 5.1 Hz, 2 H); ^{13}C NMR ($CDCl_3$, 75 MHz, ppm) δ 14.1, 22.7, 26.0, 29.2, 29.3, 29.4, 31.8, 68.0, 82.4, 113.8, 119.3, 120.3, 127.0, 129.1, 132.3, 136.0, 138.7, 139.5, 139.9, 143.9. 145.4. 158.3; MS (FAB, $M^{+\bullet}$, $C_{76}H_{94}O_6S_4$) calcd 1230.59, found 1230.

Synthesis of IDTT. To a solution of **2** (1.00 g, 0.81 mmol) in THF (100 mL) was added concentrated sulfuric acid (0.5 mL). The mixture was stirred for 2 h at 90 °C, cooled to room temperature, poured into water (250 mL), and extracted with ethyl acetate (500 mL × 3). The combined organic layer was dried over $MgSO_4$ and the solvent was removed under reduced pressure. The residue was then purified by column chromatography on silica gel (hexane/ethyl acetate, v/v, 80/1) to afford an yellow solid **IDTT** (1.58 g, 81%): ^1H NMR ($CDCl_3$, 400 MHz, ppm) δ 0.87 (t, J = 6.8 Hz, 12 H), 1.26−1.43 (m, 40 H), 1.70−1.77 (m, 8 H), 3.89 (t, J = 6.6 Hz, 8 H), 6.79 (d, J = 8.8 Hz, 8 H), 7.19 (d, J = 8.8 Hz, 8 H), 7.25−7.29 (m, 4 H), 7.45 (s, 2 H) ; ^{13}C NMR ($CDCl_3$, 75 MHz, ppm) δ 14.1, 22.6, 26.1, 29.2, 29.3, 29.3, 31.8, 62.2, 67.9, 114.3, 116.7, 120.4, 126.3, 129.2, 133.6, 134.9, 136.0, 141.7, 143.0. 146.3. 153.5. 158.2; MS (FAB, $M^{+\bullet}$, $C_{76}H_{90}O_4S_4$) calcd 1195.79, found 1195.

Synthesis of Monomer Br-IDTT. To a solution of **IDTT** (1.1 g, 0.92 mmol) in THF (30 mL) was added *N*-bromosuccinimide (0.38 g, 2.12 mmol) at room temperature. The reaction mixture, kept away from light, was stirred for 12 h at room temperature, quenched by water (50 mL + 150 mL), and extracted with ethyl acetate (150 mL × 3). The collected organic layer was dried over $MgSO_4$. After removal of the solvent under vacuum, the residue was purified by column chromatography on silica gel (hexane/ethyl acetate, v/v, 100/1) and then recrystallized from hexane to give a brown solid **Br-IDTT**(1.08 g, 87%): ^1H NMR ($CDCl_3$, 300 MHz, ppm) δ 0.88 (t, J = 6.3 Hz, 12 H), 1.27−1.42 (m, 40 H), 1.72−1.77 (m, 8 H), 3.90 (t, J = 6.5 Hz, 8 H), 6.80 (d, J = 8.6 Hz, 8 H), 7.14 (d, J = 8.6 Hz, 8 H), 7.27 (s, 2 H), 7.44 (s, 2 H); ^{13}C NMR ($CDCl_3$, 75 MHz, ppm) δ 14.1, 22.6, 26.0, 29.2, 29.3, 29.3, 31.8, 62.1, 67.9, 112.5, 114.4, 116.8, 123.1, 129.0, 133.9, 134.5, 135.8, 139.9, 142.1. 146.6. 153.6. 158.3; MS (FAB, $M^{+\cdot}$, $C_{76}H_{88}Br_2O_4S_4$) calcd 1353.58, found 1353.

Synthesis of Sn-IDTT. To a THF (30 mL) solution of **Br-IDTT** (0.85 g, 0.63 mmol) was added a hexane solution of *n*-BuLi (2.5M, 1.58 mmol) dropwise at −78 °C. The mixture was stirred at this temperature for 1 h and a THF solution of chlorotrimethylstannane (1.0 M, 1.89 mmol) was then introduced dropwise. It was quenched with water (50 mL) and extracted with ether (50 mL × 3). The collected organic layer was dried over $MgSO_4$ and the solvent was removed *in vacuo*. The residue was recrystallized from hexane to give a brown solid **Sn-IDTT**(0.52 g, 54%): ^1H NMR ($CDCl_3$, 300 MHz,

dx.doi.org/10.1021/ma3019552 | *Macromolecules* 2012, 45, 9282−9291

ppm) δ 0.37 (s, 18 H), 0.87 (t, J = 6.6 Hz, 12 H), 1.27−1.41 (m, 40 H), 1.69−1.78 (m, 8 H), 3.89(t, J = 6.6 Hz, 8 H), 6.79 (d, J = 8.7 Hz, 8 H), 7.19 (d, J = 8.7 Hz, 8 H), 7.30 (s, 2 H), 7.42 (s, 2 H); ^{13}C NMR ($CDCl_3$, 100 MHz, ppm) δ −8.1, 14.1, 22.6, 26.1, 29.2, 29.3, 29.3, 31.8, 62.1, 67.9, 114.2, 116.6, 127.4, 129.3, 135.2, 136.1, 139.1, 140.3, 143.0, 143.8. 145.8. 153.3. 158.1.

Synthesis of PIDTTBT. To a 50 mL round-bottom flask were introduced **Sn-IDTT** (200 mg, 0.131 mmol), 4,7-dibromo-2,1,3-benzothiadiazole (38.5 mg, 0.131 mmol), $Pd_2(dba)_3$ (4.8 mg, 0.005 mmol), tri(*o*-tolyl)phosphine (12.8 mg, 0.042 mmol), and dry chlorobenzene (7 mL). The mixture was bubbled with nitrogen for 10 min at room temperature. The reaction was then carried out in a microwave reactor under 270 W for 50 min. In order to end-cap the resultant polymer, tributyl(thiophen-2-yl)stannane (24.4 mg, 0.059 mmol) was added to the mixture, and the microwave reaction was continued for 10 min under 270 W. Subsequent to tributyl(thiophen-2-yl)stannane, another end-capping reagent, 2-bromothiophene (11.6 mg, 0.063 mmol), was added and the reaction was continued for another 10 min under otherwise identical conditions. The mixture was then added into methanol dropwise. The precipitate was collected by filtration and washed by Soxhlet extraction with acetone and hexane sequentially for 3 days. The crude polymer was dissolved in hot THF and the residual Pd catalyst and Sn metal in the THF solution was removed by Pd−thiol gel and Pd-TAAcOH (Silicycle Inc.). After filtration and removal of the solvent, the polymer was redissolved in THF and reprecipitated by methanol. The resultant polymer was collected by filtration and dried under vacuum for 1 day to afford a dark-purple fiber-like solid (150 mg, 84%, M_n = 16600, PDI = 1.70): ^{1}H NMR ($CDCl_3$, 300 MHz) δ 0.87 (br, 12 H), 1.26−1.42 (br, 40 H), 1.74 (br, 8 H), 3.91 (br, 8 H), 6.84 (br, 8 H), 7.19 (br, 8 H), 7.35−7.55 (m, 2 H), 7.75 (br, 2 H), 8.57 (br, 2 H).

Synthesis of PIDTTFBT. To a 50 mL round-bottom flask were introduced **Sn-IDTT** (200 mg, 0.131 mmol), 4,7-dibromo-5,6-difluoro-2,1,3-benzothiadiazole (43.2 mg, 0.131 mmol), $Pd_2(dba)_3$ (4.8 mg, 0.005 mmol), tri(*o*-tolyl)phosphine (12.8 mg, 0.042 mmol), and dry chlorobenzene (7 mL). The mixture was bubbled with nitrogen for 10 min at room temperature. The reaction was then carried out in a microwave reactor under 270 W for 50 min. In order to end-cap the resultant polymer, tributyl(thiophen-2-yl)stannane (24.4 mg, 0.059 mmol) was added to the mixture, and the microwave reaction was continued for 10 min under 270 W. Subsequent to tributyl(thiophen-2-yl)stannane, another end-capping reagent, 2-bromothiophene (11.6 mg, 0.063 mmol) was added and the reaction was continued for another 10 min under otherwise identical conditions. The mixture was then added into methanol dropwise. The precipitate was collected by filtration and washed by Soxhlet extraction with acetone and hexane sequentially for three days. The crude polymer was dissolved in hot THF and the residual Pd catalyst and Sn metal in the THF solution was removed by Pd−thiol gel and Pd−TAAcOH (Silicycle Inc.). After filtration and removal of the solvent, the polymer was redissolved in THF and reprecipitated by methanol. The resultant polymer was collected by filtration and dried under vacuum for 1 day to afford a give a dark-purple fiber-like solid (160 mg, 86%, M_n = 24000, PDI = 1.18): δ ^{1}H NMR ($CDCl_3$, 300 MHz) δ 0.86 (br, 12 H), 1.26−1.29 (br, 40 H), 1.74 (br, 8 H), 3.91 (br, 8 H), 6.84 (br, 8 H), 7.27 (br, 8 H), 7.54 (br, 2 H), 8.66 (br, 2 H).

Synthesis of PIDTTTPD. To a 50 mL round-bottom flask were introduced **Sn-IDTT** (200 mg, 0.131 mmol), 1,3-dibromo-thieno[3,4-*c*]pyrrole-4,6-dione (55.6 mg, 0.131 mmol), $Pd_2(dba)_3$ (4.8 mg, 0.005 mmol), tri(*o*-tolyl)phosphine (12.8 mg, 0.042 mmol), and dry chlorobenzene (7 mL). The mixture was bubbled with nitrogen for 10 min at room temperature. In order to end-cap the resultant polymer, tributyl(thiophen-2-yl)stannane (24.4 mg, 0.059 mmol) was added to the mixture, and the microwave reaction was continued for 10 min under 270 W. Subsequent to tributyl(thiophen-2-yl)stannane, another end-capping reagent, 2-bromothiophene (11.6 mg, 0.063 mmol) was added, and the reaction was continued for another 10 min under otherwise identical conditions. The mixture was then added into methanol dropwise. The precipitate was collected by filtration and washed by Soxhlet extraction with acetone and hexane sequentially for three days. The crude polymer was dissolved in hot THF and the residual Pd catalyst and Sn metal in the THF solution was removed by Pd−thiol gel and Pd−TAAcOH (Silicycle Inc.). After filtration and removal of the solvent, the polymer was redissolved in THF and reprecipitated by methanol. The resultant polymer was collected by filtration and dried under vacuum for 1 day to give a dark-purple fiber-like solid (170 mg, 89%, M_n = 31300, PDI = 2.04): δ ^{1}H NMR ($CDCl_3$, 300 MHz) δ 0.87 (br, 15 H), 1.27−1.43 (m, 50 H), 1.75 (br, 10 H), 3.92 (br, 10 H), 6.84 (br, 8 H), 7.19 (br, 8 H), 7.50 (br, 2 H), 8.52 (br, 2 H).

■ ASSOCIATED CONTENT

Ⓢ Supporting Information

Computational details, thermogravimetric analysis, and ^{1}H and ^{13}C NMR spectra of the new compounds and copolymers. This material is available free of charge via the Internet at http://pubs.acs.org/.

■ AUTHOR INFORMATION

Corresponding Author

*E-mail: yjcheng@mail.nctu.edu.tw.

Notes

The authors declare no competing financial interest.

■ ACKNOWLEDGMENTS

We thank the National Science Council and the "ATU Program" of the Ministry of Education, Taiwan, for financial support. We are also grateful to the National Center for High-performance Computing (NCHC) in Taiwan for computer time and facilities.

■ REFERENCES

(1) Yu, G.; Gao, J.; Hummelen, J. C.; Wudl, F.; Heeger, A. J. *Science* **1995**, *270*, 1789.

(2) (a) Thompson, B. C.; Fréchet, J. M. J. *Angew. Chem., Int. Ed.* **2008**, *47*, 58. (b) Cheng, Y.-J.; Yang, S.-H.; Hsu, C.-S. *Chem. Rev.* **2009**, *109*, 5868. (c) Chen, J.; Cao, Y. *Acc. Chem. Res.* **2009**, *42*, 1709. (d) Li, Y.; Zou, Y. *Adv. Mater.* **2008**, *20*, 2952. (e) Li, Y. *Acc. Chem. Res.* **2012**, *45*, 723. (f) Huo, L.; Hou, J. *Polym. Chem.* **2011**, *2*, 2453. (g) Duan, C.; Huang, F.; Cao, Y. *J. Mater. Chem.* **2012**, *22*, 10416. (h) Zhou, H.; Yang, L.; You, W. *Macromolecules* **2012**, *45*, 607.

(3) (a) Svensson, M.; Zhang, F.; Veenstra, S. C.; Verhees, W. J. H.; Hummelen, J. C.; Kroon, J. M.; Inganäs, O.; Andersson, M. R. *Adv. Mater.* **2003**, *15*, 988. (b) Zhou, Q.; Hou, Q.; Zheng, L.; Deng, X.; Yu, G.; Cao, Y. *Appl. Phys. Lett.* **2004**, *84*, 1653. (c) Zhang, F.; Mammo, W.; Andersson, L. M.; Admassie, S.; Andersson, M. R.; Inganäs, O. *Adv. Mater.* **2006**, *18*, 2169. (d) Zhang, F.; Bijleveld, J.; Perzon, E.; Tvingstedt, K.; Barrau, S.; Inganäs, O.; Andersson, M. R. *J. Mater. Chem.* **2008**, *18*, 5468. (e) Schulz, G. L.; Chen, X.; Holdcroft, S. *Appl. Phys. Lett.* **2009**, *94*, 023302. (f) Huang, F.; Chen, K.-S.; Yip, H.-L.; Hau, S. K.; Acton, O.; Zhang, Y.; Luo, J.; Jen, A. K.-Y. *J. Am. Chem. Soc.* **2009**, *131*, 13886.

(4) (a) Zhu, Z.; Waller, D.; Gaudiana, R.; Morana, M.; Mühlbacher, D.; Scharber, M.; Brabec, C. *Macromolecules* **2007**, *40*, 1981. (b) Mühlbacher, D.; Scharber, M.; Zhengguo, M. M.; Zhu, M. M. Z.; Waller, D.; Gaudiana, R.; Brabec, C. *Adv. Mater.* **2006**, *18*, 2884. (c) Kim, J. Y.; Lee, K.; Coates, N. E.; Moses, D.; Nguyen, T.-Q.; Dante, M.; Heeger, A. J. *Science* **2007**, *317*, 222. (d) Peet, J.; Kim, J. Y.; Coates, N. E.; Ma, W. L.; Moses, D.; Heeger, A. J.; Bazan, G. C. *Nat. Mater.* **2007**, *6*, 497. (e) Chen, C.-H.; Hsieh, C.-H.; Dubosc, M.; Cheng, Y.-J.; Hsu, C.-S. *Macromolecules* **2010**, *43*, 697.

(5) (a) Li, Y.; Wu, Y.; Liu, P.; Birau, M.; Pan, H.; Ong, B. S. *Adv. Mater.* **2006**, *18*, 3029. (b) McCulloch, I.; Heeney, M.; Bailey, C.; Genevicius, K.; MacDonald, I.; Shkunov, M.; Sparrowe, D.; Tierney, S.; Wagner, R.; Zhang, W.; Chabinyc, M. L.; Kline, R. J.; Mcgehee, M. D.; Toney, M. F. *Nat. Mater.* **2006**, *5*, 328.

(6) (a) Subramanian, G.; Schleyer, P. R.; Jiao, H. *Angew. Chem., Int. Ed. Engl.* **1996**, *35*, 2638. (b) Hess, B. A., Jr.; Schaad, L. J. *J. Am. Chem. Soc.* **1973**, *95*, 3907.
(7) (a) Hayashi, N.; Mazaki, Y.; Kobayashi, K. *J. Chem. Soc., Chem. Commun.* **1994**, 2351. (b) DeLongchamp, D. M.; Kline, R. J.; Lin, E. K.; Fischer, D. A.; Richter, L. J.; Lucas, L. A.; Heeney, M.; McCulloch, I.; Northrup, J. E. *Adv. Mater.* **2007**, *19*, 833. (c) Chabinyc, M. L.; Toney, M. F.; Kline, R. J.; McCulloch, I.; Heeney, M. *J. Am. Chem. Soc.* **2007**, *129*, 3226.
(8) (a) Zhang, X.; Kohler, M.; Matzger, A. J. *Macromolecules* **2004**, *37*, 6306. (b) Miguel, L. S.; Matzger, A. J. *Macromolecules* **2007**, *40*, 9233. (c) Miguel, S, L.; Matzger, A, J. *J. Org. Chem.* **2007**, *72*, 442. (d) Henssler, J, T.; Zhang, X.; Matzger, A, J. *J. Org. Chem.* **2009**, *74*, 9112.
(9) (a) Liang, Y.; Wu, Y.; Feng, D.; Tsai, S.-T.; Son, H.-J.; Li, G.; Yu, L. *J. Am. Chem. Soc.* **2009**, *131*, 56. (b) He, F.; Wang, W.; Chen, W.; Xu, T.; Darling, S. B.; Strzalka, J.; Liu, Y.; Yu, L. *J. Am. Chem. Soc.* **2011**, *133*, 3284. (c) Zhang, Y.; Zou, J.; Yip, H.-L.; Chen, K.-S.; Zeigler, D. F.; Sun, Y.; Jen, A. K.-Y. *Chem. Mater.* **2011**, *23*, 2289. (d) Cheng, Y.-J.; Wu, J.-S.; Shih, P.-I.; Chang, C.-Y.; Jwo, P.-C.; Kao, W.-S.; Hsu, C.-S. *Chem. Mater.* **2011**, *23*, 2361. (e) Wu, J.-S.; Cheng, Y.-J.; Dubosc, M.; Hsieh, C.-H.; Chang, C.-Y.; Hsu, C.-S. *Chem. Commun.* **2010**, *46*, 3259. (f) Wu, J.-S.; Cheng, Y.-J.; Lin, T.-Y.; Chang, C.-Y.; Shih, P.-I.; Hsu, C.-S. *Adv. Funct. Mater.* **2012**, *22*, 1711. (g) Wang, J.-Y.; Hau, S. K.; Yip, H.-L.; Davies, J. A.; Chen, K.-S.; Zhang, Y.; Sun, Y.; Jen, A. K.-Y. *Chem. Mater.* **2011**, *23*, 765. (h) Ashraf, R. S.; Chen, Z.; Leem, D. S.; Bronstein, H.; Zhang, W.; Schroeder, B.; Geerts, Y.; Smith, J.; Watkins, S.; Anthopoulos, T. D.; Sirringhaus, H.; Mello, J. C.; de; Heeney, M.; McCulloch, I. *Chem. Mater.* **2011**, *23*, 768. (i) Chen, C.-H.; Cheng, Y.-J.; Dubosc, M.; Hsieh, C.-H.; Chu, C.-C.; Hsu, C.-S. *Chem. Asian. J.* **2010**, *5*, 2480. (j) Zhang, M.; Guo, X.; Wang, X.; Wang, H.; Li, Y. *Chem. Mater.* **2011**, *23*, 4264. (k) Cheng, Y.-J.; Chen, C.-H.; Lin, Y.-S.; Chang, C.-Y.; Hsu, C.-S. *Chem. Mater.* **2011**, *23*, 5068. (l) Chen, C.-H.; Cheng, Y.-J.; Chang, C.-Y.; Hsu, C.-S. *Macromolecules* **2011**, *44*, 8415. (m) Cheng, Y.-J.; Ho, Y.-J.; Chen, C.-H.; Kao, W.-S.; Wu, C.-E.; Hsu, S.-L.; Hsu, C.-S. *Macromolecules* **2012**, *45*, 2690. (n) Chen, Y. -C.; Yu, C. -Y.; Fan, Y.-L.; Huang, L.-I.; Chen, C.-P.; Ting, C. *Chem. Commun.* **2010**, *46*, 6503. (o) Zhang, Y.; Zou, J.; Yip, H.-L.; Chen, K.-S.; Davies, J. A.; Sun, Y.; Jen, A. K. Y. *Macromolecules* **2011**, *44*, 4752.
(10) (a) Goldfinger, M. B.; Crawford, K. B.; Swager, T. M. *J. Am. Chem. Soc.* **1997**, *119*, 4578. (b) Goldfinger, M. B.; Swager, T. M. *J. Am. Chem. Soc.* **1994**, *116*, 7895. (c) Forster, M.; Annan, K. O.; Scherf, U. *Macromolecules* **1999**, *32*, 3159. (d) Scherf, U. *J. Mater. Chem.* **1999**, *9*, 1853. (e) Chmil, K.; Scherf, U. *Acta Polym.* **1997**, *48*, 208. (f) Jacob, J.; Sax, S.; Piok, T.; List, E. J. W.; Grimsdale, A. C.; Mullen, K. *J. Am. Chem. Soc.* **2004**, *126*, 6987. (g) Zheng, Q.; Jung, B. J.; Sun, J.; Katz, H. E. *J. Am. Chem. Soc.* **2010**, *132*, 5394. (h) Facchetti, A. *Chem. Mater.* **2011**, *23*, 733. (i) Guo, X.; Ortiz, R. P.; Zheng, Y.; Hu, Y.; Noh, Y.-Y.; Baeg, K.-J.; Facchetti, A.; Marks, T. J. *J. Am. Chem. Soc.* **2011**, *133*, 1405. (j) Cheng, Y.-J.; Ho, Y.-J.; Chen, C.-H.; Kao, W.-S.; Wu, C.-E.; Hsu, S.-L.; Hsu, C.-S. *Macromolecules* **2012**, *45*, 2690. (k) Chang, C.-Y.; Cheng, Y.-J.; Hung, S.-H.; Wu, J.-S.; Kao, W.-S.; Lee, C.-H.; Hsu, C.-S. *Adv. Mater.* **2012**, *24*, 549.
(11) Cheng, Y.-J.; Cheng, S.-W.; Chang, C.-Y.; Kao, W.-S.; Liao, M.-H.; Hsu, C.-S. *Chem. Commun.* **2012**, *48*, 3203.
(12) (a) Boudreault, P.-L. T.; Najari, A.; Leclerc, M. *Chem. Mater.* **2011**, *23*, 456. (b) Peng, Q.; Liu, X.; Su, D.; Fu, G.; Xu, J.; Dai, L. *Adv. Mater.* **2011**, *23*, 4554. (c) Hou, J. H.; Chen, H. Y.; Zhang, S. Q.; Yang, Y. *J. Phys. Chem. C* **2009**, *113*, 21202. (d) Wang, X. C.; Sun, Y. P.; Chen, S.; Guo, X.; Zhang, M. J.; Li, X. Y.; Li, Y.; Wang, H. Q. *Macromolecules* **2012**, *45*, 1208.
(13) (a) Nielsen, C. B.; Bjørnholm, T. *Org. Lett.* **2004**, *6*, 3381. (b) Chen, C. M.; Amb., S.; Graham, K. R.; Subbiah, J.; Small, C. E.; So, F.; Reynolds, J. R. *J. Am. Chem. Soc.* **2011**, *133*, 10062. (c) Chu, T. Y.; Lu, J.; Beaupré, S.; Zhang, Y.; Pouliot, J. R.; Wakim, S.; Zhou, J.; Leclerc, M.; Li, Z.; Ding, J.; Tao, Y. *J. Am. Chem. Soc.* **2011**, *133*, 4250. (d) Berrouard, P.; Najari, A.; Pron, A.; Gendron, D.; Morin, P.-O.; Pouliot, J.-R.; Veilleux, J.; Leclerc, M. *Angew. Chem., Int. Ed.* **2012**, *51*, 2068. (e) Zou, Y.; Najari, A.; Berrouard, P.; Beaupré, S.; Aïch, B. R.; Tao, Y.; Leclerc, M. *J. Am. Chem. Soc.* **2010**, *132*, 5330. (f) Zhang, Y.; Hau, S. K.; Yip, H. L.; Sun, Y.; Acton, O.; Jen, A. K. Y. *Chem. Mater.* **2010**, *22*, 2696. (g) Piliego, C.; Holcombe, T. W.; Douglas, J. D.; Woo, C. H.; Beaujuge, P. M.; Fréchet, J. M. J. *J. Am. Chem. Soc.* **2010**, *132*, 7595. (h) Najari, A.; Beaupré, S.; Berrouard, P.; Zou, Y.; Pouliot, J. R.; Pérusse, C. L.; Leclerc, M. *Adv. Funct. Mater.* **2011**, *21*, 718.
(14) (a) Zhang, Y.; Chien, S.-C.; Chen, K.-S.; Yip, H.-L.; Sun, Y.; Davies, J. A.; Chen, F.-C.; Jen, A. K. Y. *Chem. Commun.* **2011**, *47*, 11026. (b) Zhou, H.; Yang, L.; Stuart, A. C.; Price, S. C.; Liu, S.; You, W. *Angew. Chem., Int. Ed.* **2011**, *50*, 2995. (c) Schroeder, B. C.; Huang, Z.; Ashraf, R. S.; Smith, J.; D'Angelo, P.; Watkins, S. E.; Anthopoulos, T. D.; Durrant, J. R.; McCulloch, I. *Adv. Funct. Mater.* **2012**, *22*, 1663. (d) Li, Z.; Lu, J.; Tse, S.-C.; Zhou, J.; Du, X.; Tao, Y.; Ding, J. *J. Mater. Chem.* **2011**, *21*, 3226.
(15) O'Boyle, N. M.; Tenderholt, A. L.; Langner., K. M. *J. Comput. Chem.* **2008**, *29*, 839.